

# Highly conductive epoxy/graphite composites for bipolar plates in proton exchange membrane fuel cells

Ling Du, Sadhan C. Jana\*

*Department of Polymer Engineering, University of Akron, 250 South Forge Street, Akron, OH 44325-0301, USA*

Received 15 March 2007; received in revised form 17 May 2007; accepted 17 May 2007

Available online 26 May 2007

## Abstract

Carbon-filled epoxy composites are developed for potential application as bipolar plates in proton exchange membrane (PEM) fuel cells. These composites are prepared by solution intercalation mixing, followed by compression molding and curing. Electrical conductivity, thermal and mechanical properties, and hygrothermal characteristics are determined as function of carbon-filler content. Expanded graphite and carbon black are used as synergistic combination to obtain desired in-plane and through-plane conductivities. These composites show high glass transition temperatures ( $T_g \sim 180^\circ\text{C}$ ), high thermal degradation temperatures ( $T_2 \sim 415^\circ\text{C}$ ), in-plane conductivity of  $200\text{--}500\text{ S cm}^{-1}$  with 50 wt% carbon fillers, in addition to offering high values of flexural modulus, flexural strength, and impact strength, respectively  $2 \times 10^4\text{ MPa}$ ,  $72\text{ MPa}$ , and  $173\text{ J m}^{-1}$ . The presence of carbon fillers helps reduce water uptake from 4 to 5 wt% for unfilled epoxy resins to 1–2 wt%. In addition, morphology, electrical, mechanical, and thermal properties remain unchanged on exposure to boiling water and acid reflux. This data indicate that the composites developed in this work meet many attributes of bipolar plates for use in PEM fuel cells.

© 2007 Elsevier B.V. All rights reserved.

**Keywords:** Bipolar plates; Graphite-epoxy composite; Electrical conductivity; Hygrothermal effects

## 1. Introduction

Proton exchange membrane (PEM) fuel cells are considered a promising candidate for zero-emission power source required for environmentally friendly transportation and stationary applications. High efficiency and power density, low operating temperature, and quick startup make PEM fuel cells very attractive in applications requiring from a few watts to megawatts, including power supplies in cellular telephones, laptop computers and portable entertainment equipment, automobiles, and military communication installations [1–4].

The bipolar plate is a multifunctional component within the PEM fuel cell stack. It serves the following functions: (i) connect and separate the individual fuel cells in series to form a fuel cell stack with required voltage; (ii) aid uniform distribution of fuel gas and oxygen over the whole active surface area of the membrane-electrode assemblies (MEA); (iii) conduct electrical current from the anode of one cell

to the cathode of the next; (iv) facilitate water management within the cell; (v) enable heat transfer; (vi) support thin membrane and electrodes and clamping forces for the stack assembly. The composite bipolar plates should meet the following requirements: (a) high in-plane electrical conductivity ( $>100\text{ S cm}^{-1}$ ), and low area specific resistance ( $<30\text{ m}\Omega\text{ cm}^2$ ) [5]; (b) chemical stability in the presence of hydrogen fuel, oxygen, and slightly acidic water ( $\text{pH} < 4$ ), corrosion resistance  $<16\text{ }\mu\text{A cm}^{-2}$  [5]; (c) chemical compatibility, such as no byproducts affecting the MEA performance and no plate surface degradations; (d) high thermal conductivity,  $>10\text{ W (mK)}^{-1}$  [6]; (e) low permeability to hydrogen and oxygen with hydrogen permeability  $<2 \times 10^{-6}\text{ cm}^3\text{ cm}^{-2}\text{ s}^{-1}$  [5]; (f) good mechanical properties, such as, tensile strength  $>41\text{ MPa}$ , flexural strength  $>59\text{ MPa}$ , impact strength  $>40.5\text{ J m}^{-1}$ ; crush strength  $>4200\text{ kPa}$  [5,6]; (g) thermal stability at fuel cell operating temperatures ( $-40\text{--}120^\circ\text{C}$ ).

The polymer composite materials, such as the ones developed in this work can alleviate some of the concerns related to weight and volume, and hence the cost of fuel cell stacks. Conventional pure graphite bipolar plates contribute significantly to the cost and weight of PEM fuel cell stacks. Metals such

\* Corresponding author. Tel.: +1 330 972 8293; fax: +1 330 258 2339.  
E-mail address: [janas@uakron.edu](mailto:janas@uakron.edu) (S.C. Jana).

as stainless steel and metal alloys – alternatives favored by industry – are not preferable because of corrosion related issues [7,8], although coatings by carbon film [9], polypyrrole [10], gold [11], and chromium nitrides [12] have been found useful. In view of this, development of lightweight, low cost and highly conductive polymer composite bipolar plates with scope for mass production can aid rapid commercialization of PEM fuel cells [2,4,13]. Such polymer composite bipolar plate can replace heavier graphite bipolar plate in next generation PEM fuel cells. Both thermoplastic and thermosetting resins have been considered for development of carbon-based composite bipolar plates [2,14,15,3,16–18]. Researchers at Oak Ridge National Laboratory developed carbon/carbon composite bipolar plates with in-plane electrical conductivity of 200–300 S cm<sup>-1</sup> and excellent mechanical properties, although the process was found to be somewhat complicated and costly for certain applications such as automotives [19]. Kuo and Chen [20] developed bipolar plates using 40 wt% polyamide 6 and 60 wt% stainless steel alloy fibers. Baird and coworkers [2,13,18] developed graphite-based wet-lay composite bipolar plates of polyphenylenesulphide (PPS) and reported in-plane conductivity higher than 200 S cm<sup>-1</sup> and through-plane conductivity of 19 S cm<sup>-1</sup>. It is imperative that higher through-plane conductivity is needed to meet the requirements mentioned above.

In this study, carbon-filled thermosetting epoxy composites were investigated as an alternative material for bipolar plates to meet the US Department of Energy (DOE) targets on both in-plane and through-plane conductivity, and to offer mechanical integrity at temperatures higher than 150 °C. The high in-plane and through-plane conductivities were obtained from the synergistic effects of highly conductive expanded graphite (EG) and carbon black (CB) particles without compromise on mechanical properties. Several studies investigated electrical conduction in polymer/EG composites [21,22], although the loading of EG in these studies were restricted to less than 5 wt%. In the current study, however, the total filler loading was maintained at greater than 50 wt% to obtain desired level of conductivity.

It is imperative that the polymer matrix should offer desired chemical stability and mechanical integrity against acid environment as polymeric bipolar plates come in contact with oxidant and are used in acidic environment (pH < 4.0) for an extended period of time. In view of this, the hygrothermal properties of the composites were evaluated in this study.

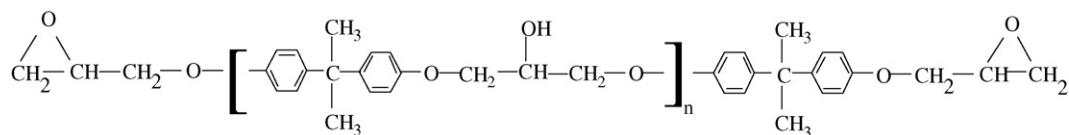
## 2. Experimental

### 2.1. Materials

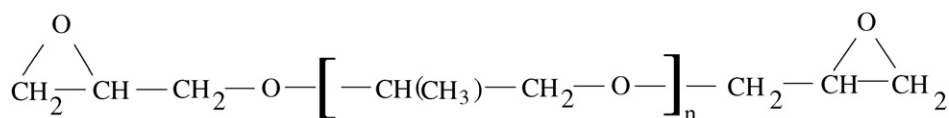
The composite materials were synthesized from a mixture of an aromatic and an aliphatic epoxy resins. The aromatic epoxy was diglycidyl ether of bisphenol A (DGEBA) in the form of Epon<sup>®</sup> 826, which was obtained from Resolution Performance Products (Houston, TX) with epoxide equivalent weight of 178–186, viscosity of 65–95 Pa s, and specific gravity of 1.15 at 25 °C. The aliphatic epoxy was polypropyleneglycol glycidyl ether in the form of Araldite<sup>®</sup> DY3601, received from Vantico (Brewster, NY) with epoxide equivalent weight of 385–405, viscosity of 0.42–0.52 Pa s, and specific gravity of 1.03 at 25 °C. Epon<sup>®</sup> 826 and Araldite<sup>®</sup> DY3601 were mixed in the ratio of 100:0, 90:10, 80:20, and 70:30 by weight—these composites will be denoted as EP100, EP90, EP80, and EP70, respectively. In this study, a majority of composites was prepared using EP90 formulation of aromatic and aliphatic epoxies. The curing agent, diaminodiphenylsulphone (DDS) was received from Ciba (Tarrytown, NY) with trade name HT976, melting temperature 180 °C and molecular weight 248 g mol<sup>-1</sup>. Epon<sup>®</sup> 826 cured with DDS produced a brittle material, while Araldite DY3601<sup>®</sup> cured with DDS produced a gum-like material. On the other hand, the mixture of 10 wt% Araldite<sup>®</sup> DY3601 with Epon<sup>®</sup> 826 (EP90) yielded more ductile material when cured with DDS. The structures of epoxy resins and curing agent are presented in Table 1. Electrically conductive carbon black (CB), Ketjenblack<sup>®</sup> EC-600 JD was received from Akzo Nobel Chemicals Inc. (Chicago, IL). Expandable graphite (EG),

Table 1  
Structures of epoxy resins and curing agent

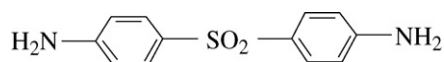
Epon<sup>®</sup> 826: diglycidyl ether of bisphenol A (DGEBA);  $n = 0.085$



Araldite<sup>®</sup> DY3601: polypropylene glycol diglycidyl ether;  $n = 11.4$



DDS: diaminodiphenylsulphone, MW = 248 g/mol



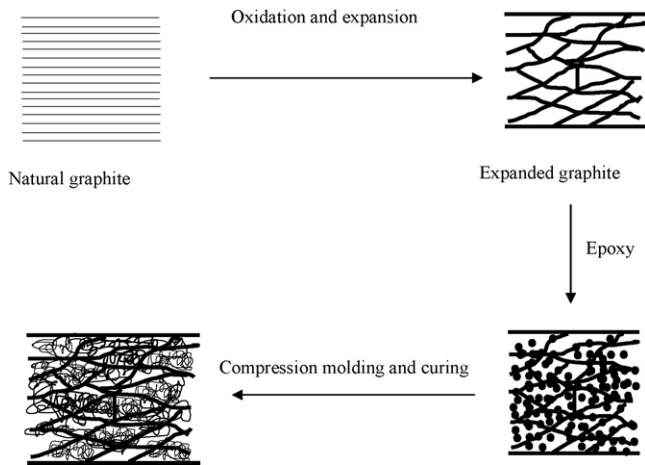


Fig. 1. Schematic diagram showing stages in preparation of composites.

GRAFGUARD® Expanding Flake 160–50 N with high expansion volume of  $\sim 250 \text{ cm}^3 \text{ g}^{-1}$  at  $600^\circ\text{C}$  was obtained from GrafTech (Cleveland, OH).

## 2.2. Preparation of composites

Various epoxy resin mixtures were prepared by mixing desired quantities of Epon® 826 and Araldite® DY3601 in a beaker at room temperature, followed by addition of 5 wt% excess of curing agent DDS than necessary to balance the stoichiometry of epoxide and amine groups. Clear solutions were obtained by heating the mixtures up to  $135^\circ\text{C}$  with stirring. Alternatively, the epoxy-curing agent mixtures were prepared by adding all three components into a beaker, followed by addition of acetone as a solvent.

Composites of EG and CB were prepared by solution intercalation method, whereby expanded graphite and carbon black were added to the solution of epoxy resins and curing agent in acetone. The materials were mechanically stirred for 6 h, and the solvent was evaporated with continuous stirring. The traces of solvent were removed by keeping the materials in a vacuum oven for 24 h at  $60^\circ\text{C}$ , and 2 h at  $110^\circ\text{C}$ . The dried materials were obtained in powder form and were compression molded at a pressure of 4000 psi and  $180^\circ\text{C}$  and cured for 4–6 h, followed by post curing in vacuum oven at  $200^\circ\text{C}$  for 6 h. The total filler content in the mixture ranged from 40 to 70 wt%, with a maximum of 5 wt% CB. The composite preparation procedure and various stages of intercalation between epoxy resins and expanded graphite and carbon black particles are schematically presented in Fig. 1. Specimens for measurement of electrical conductivity and mechanical properties were cut from the compression molded sheets.

## 2.3. Measurement of in-plane and through-plane electrical conductivity

The in-plane electrical conductivity was measured by following ASTM D257-99, through conventional four point probe conductivity measurement device (Fig. 2a). The through-plane

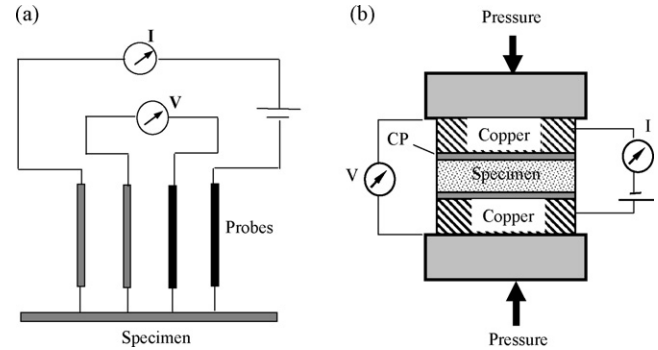


Fig. 2. Experimental setup for measuring (a) in-plane conductivity and (b) through-plane conductivity with four-point probe method. The applied voltage and measured current are respectively  $V$  and  $I$ . CP represents carbon paper.

electrical conductivity of the composites is more important to qualify the composites as bipolar plates. This was measured by using a fixture designed in our laboratory whereby the specimen were kept under pressure in the measurement setup (Fig. 2b). The through-plane resistance of the whole system depends on several resistances in series, including the resistance of two copper electrodes, two carbon paper layers, the bulk resistance of the specimen, and more significantly, the contact resistance between the carbon paper layers and the electrodes and between the carbon paper layers and the specimen. A calibration method was, therefore, used to separately measure the value of bulk resistance of the specimen and the resistance of the overall system, including specimen, carbon papers, and the contact resistances. Fig. 3 presents schematic of the set ups used in the calibration method. In Setup 1, the system resistance ( $R_{\text{Setup 1}}$ ) of one carbon paper (CP) placed between two copper electrodes was measured, while in Setup 2, the resistance measured ( $R_{\text{Setup 2}}$ ) included the resistance of two copper electrodes, two CP layers, and the bulk resistance of the specimen, and the contact resistances. Assuming that all contact resistances were the same, the bulk resistance of the specimen can be calculated by using Eq. (1):

$$R = R_{\text{Setup 2}} - 2R_{\text{Setup 1}} \quad (1)$$

where  $R$  is the resistance of the composite specimen. Once the value of resistance of the specimen was obtained, the values of conductivity were calculated using the known values of contact area and the specimen thickness. The performance of the composites for through-plane electrical conductivity via bipolar plates was also evaluated from the measurement of area specific resistance of the whole setup in Fig. 2b.

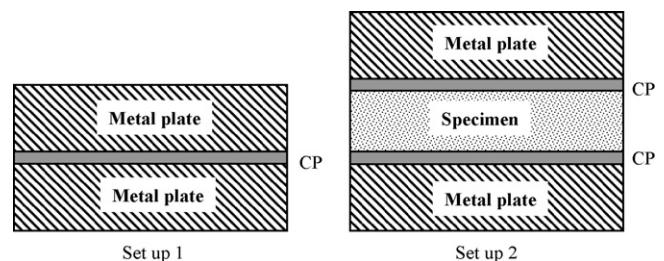


Fig. 3. Calibration setup used for measurement of through-plane conductivity. CP represents carbon paper.

## 2.4. Mechanical properties

The flexural, impact, and tensile properties were measured according to respectively ASTM D790–03, ASTM D 4812–99, and ASTM D 638–84 methods.

## 2.5. Evaluation of hygrothermal effects

Hygrothermal effects on the properties of the epoxy composite materials were investigated by exposing composite specimen for long periods of time to boiling water and sulphuric acid solution. The pH value of sulphuric acid solution was maintained between 1 and 2. The specimens were kept in boiling water and boiling acid solution in a round bottom flask fitted with a condenser. The pH of the acid solution was periodically checked and adjusted.

## 2.6. Morphology

The morphology of the epoxy composites was characterized by scanning electron microscope (SEM) (Hitachi S-2150) with the sputter coating of a layer of silver.

## 2.7. Thermal properties

The glass transition temperature ( $T_g$ ) of the composites was determined by differential scanning calorimetry (DSC) using TA Instruments, DSC 2920 system. In addition, thermogravimetric analyzer (TGA), TA Instruments, TGA 2050 was used to measure the thermal degradation temperatures, such as  $T_1$  and  $T_2$ . The values of  $T_1$  and  $T_2$  were determined from the TGA curves respectively at 5% weight loss and at maximum rate of weight loss.

## 3. Results and discussion

### 3.1. In-plane electrical conductivity of composites

The in-plane electrical conductivity was largely influenced by the total filler content as well as the filler type and the degree of filler dispersion in the polymer matrix. In Fig. 4, CB content was fixed at 5 wt%, and EG content was increased up to 85 wt%. It is seen that the conductivity of epoxy composites increased with the increase of EG content. The conductivity increased monotonically with the increase of filler content up to  $600 \text{ S cm}^{-1}$  for 75 wt%, and then jumped sharply to above  $1000 \text{ S cm}^{-1}$  at 85 wt% EG. The very high electrical conductivity of larger than  $1000 \text{ S cm}^{-1}$  at 85 wt% can be attributed to physical contacts between the filler particles, which established large numbers of electron conducting pathways. One can argue that EG content as high as 85 wt% should be used to capitalize on very high values of electrical conductivity. However, the mechanical properties were found to be poor when the content of EG was greater than 65 wt%. It was found that compression molded laminates with filler content greater than 70 wt% were fragile and in some case can be fractured easily with the application of small load by

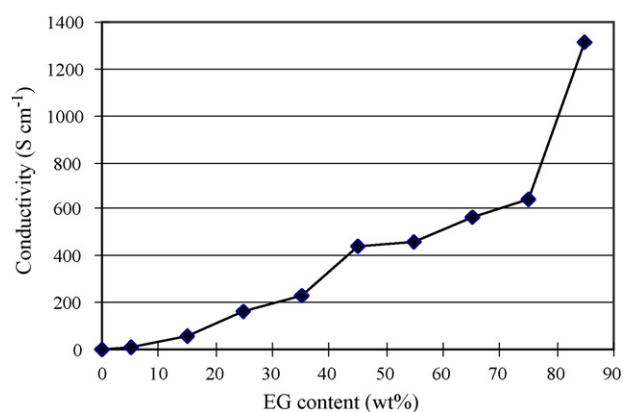


Fig. 4. In-plane conductivity of EP90 composites as function of EG content. The amount of CB was 5 wt%. Solid lines joining data points are meant to guide the eye.

hand. In view of this, we focused in this study on composites containing 35–65 wt% EG and a maximum of 5 wt% CB.

Next, in-plane electrical conductivity of EP90 composites without CB was measured and compared with that of EP90 composites with 5 wt% CB, as shown in Fig. 5. It is seen that composites with 5 wt% CB provided higher conductivities over those without CB at the same total filler loading. This indicates that CB particles effectively formed additional conductive networks in the composites. This is counter intuitive, as the intrinsic conductivity of EG is much higher than that of CB and the presence of CB particles should have lowered the overall conductivity instead of increasing it. This can be interpreted in terms of a positive synergistic effect between EG and CB on electrical conductivity. The same positive synergistic effect on electrical conductivity was observed for other epoxy mixtures. Clingerman et al. [23] also noticed positive synergistic effects using a combination of CB, synthetic graphite, and carbon fiber.

The synergistic effect can be explained on the basis of additional conductive pathways formed in the presence of CB particles. Note that the intrinsic conductivity of EG is around  $10^5 \text{ S cm}^{-1}$  and that of CB is between 10 and  $100 \text{ S cm}^{-1}$ . Nevertheless, the macroscopic resistance of polymer composites

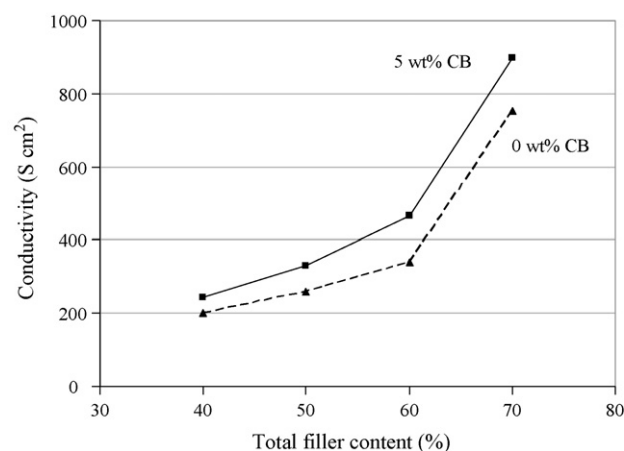


Fig. 5. In-plane conductivity of EP90 composites as function of total filler content. Lines joining data points are meant to guide the eye.

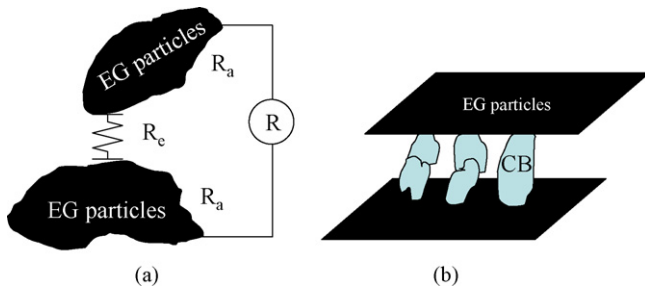


Fig. 6. Schematic illustration of (a) how various resistances act in series and define the overall resistance,  $R$  and (b) CB particles placed between two graphite platelets to help reduce the value of  $R_e$ .

depends on two contributions [24]: (1) the resistance of aggregates,  $R_a = \rho_i/d$ , where  $\rho_i$  is the resistivity of the filler, and  $d$  is the diameter of the contact area; (2) the resistance of the inter-aggregate space  $R_e$ , which results from the tunneling resistance. An expression of  $R_e$  can be written as  $R_e = \rho_t/A$ , where  $\rho_t$  is the tunneling resistivity, and  $A$  is the contact surface area of the particles. The total resistance of the composite,  $R$ , is the sum of all aggregate resistances  $R_{a,i}$  and inter-aggregate space resistances  $R_{e,i}$ , and given as

$$R = \sum R_{a,i} + \sum R_{e,i} \quad (2)$$

Fig. 6 schematically shows how various resistances contribute to the total resistance of the composites. The resistance of EG particles is very small owing to high value of intrinsic conductivity. In this case, therefore, the total resistance comes primarily from the resistance of the inter-aggregate space,  $R_e$  (Fig. 6a). Accordingly, CB particles, present in the composites, provided additional connections between EG layers, thus reducing the value of  $R_e$ , and hence the total resistance,  $R$  (Fig. 6b). Note also that CB can efficiently impart electrical conductivity with a minimum loading because of highly branched and hollow structures, high surface area, and small aggregate sizes. An evidence of the structural arrangement of EG and CB particles included in the resistivity model in Fig. 6 can be obtained from the SEM images presented in Fig. 7. These SEM images clearly show that CB particles uniformly distributed in epoxy/EG/CB com-

posites, and that many CB aggregates were present between graphite layers (Fig. 7b), thus imparting both high in-plane and through-plane conductivity between adjacent graphite layers. In this manner,  $R_e$  was substantially reduced, resulting in a lower total resistance or higher total conductivity of the composites.

### 3.2. Through-plane electrical conductivity and area specific resistance

The through-plane electrical conductivity changed only slightly in the presence of CB particles, e.g. from  $77 \text{ S cm}^{-1}$  for composite EP90/EG/CB (50/50/0) to  $79 \text{ S cm}^{-1}$  for composite EP90/EG/CB (50/45/5). Recall that the numbers in the parenthesis represent parts by weight of components in the composites. Such small contribution to through-plane conductivity by the synergistic combination of fillers is counter-intuitive in view of large enhancements observed in the case of in-plane electrical conductivity (Fig. 5). This can be attributed to large contact resistances encountered during measurements (see Figs. 2b and 3). Specifically, the resistance of Setup 1 was found to be very close to that of Setup 2 in Fig. 3, apparently due to significant contributions from the contact resistances of four contact surfaces. In view of this, we felt that a better way to characterize the through-plane electrical performance of the composite materials was to measure the values of area specific resistance using Setup 2 in Fig. 3. An area specific resistance of less than  $30 \text{ m}\Omega \text{ cm}^2$  has been accepted to minimize the voltage losses in a stack contributed by the bipolar plates [25]. Typically industrial fuel cell stack prototypes operate at a current density between 1 and  $2 \text{ A cm}^{-2}$ , and a surface area between 200 and  $400 \text{ cm}^2$ . Using these typical numbers, the voltage drop per plate can be calculated in the range from 30 to 60 mV. In our study, the area specific resistances of the system, including two copper electrodes, two CP layers, and one bipolar plate (as shown in Fig. 2b), were measured at different pressure, as shown Table 2. All composites developed in this study have area specific resistance less than  $30 \text{ m}\Omega \text{ cm}^2$ . In view of this, the voltage loss for these composites falls in the range from 20 to 40 mV. This compares favorably to a voltage drop of  $50 \text{ mV cell}^{-1}$  for a well-humidified  $100 \mu\text{m}$  thick Nafion<sup>®</sup> membrane operated at  $1 \text{ A cm}^{-2}$  [26,27].

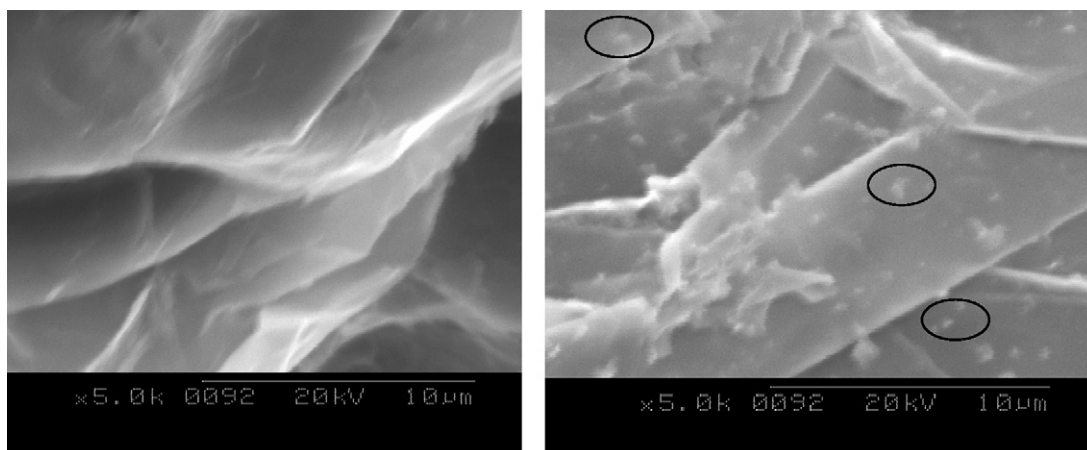


Fig. 7. SEM images of (a) EP90/EG/CB (50/50/0), (b) EP90/EG/CB (50/45/5). The granular images inside circles in (b) indicate CB particles.

Table 2

Area specific resistance (ASR) of EP90 composites at different assembly pressures

EP/EG/CB	ASR ( $\text{m}\Omega \text{cm}^2$ ) (1000 psi)	ASR ( $\text{m}\Omega \text{cm}^2$ ) (2000 psi)
50/50/0	21	13
50/45/5	12	11
40/60/0	18	16
40/55/5	17	16

Table 3

Glass transition and thermal degradation temperatures of epoxy resins

Epoxy	$T_g$ ( $^{\circ}\text{C}$ )	$T_1$ ( $^{\circ}\text{C}$ )	$T_2$ ( $^{\circ}\text{C}$ )
EP100	201	390	424
EP90	182	400	425
EP80	111	395	430
EP70	99	381	410

### 3.3. Thermal stability

Glass transition temperatures and thermal degradation temperatures  $T_1$  and  $T_2$  of epoxy resins and composites were measured using DSC and TGA, respectively, as presented in Tables 3 and 4. It is seen that thermal degradation temperatures  $T_1$  of all epoxy resins and composites are higher than  $360^{\circ}\text{C}$ , and  $T_2$  are higher than  $400^{\circ}\text{C}$ . The glass transition temperatures of EP100 and EP90 composites are around  $180^{\circ}\text{C}$ , which is much higher than  $140^{\circ}\text{C}$ , the highest PEM hydrogen fuel cell operating temperature. These data indicate that EP100 and EP90 composites are thermally and dimensionally stable at the operating temperatures of PEM hydrogen fuel cells. However, the glass transition temperatures of EP80 and EP70 are lower than  $140^{\circ}\text{C}$ . In view of this, these two epoxy systems were excluded from further investigation.

### 3.4. Hygrothermal effect

As bipolar plates are continuously used in acidic environment at high temperature ( $<140^{\circ}\text{C}$ ) and at high humidity, it is crucial to evaluate the effects of these conditions on electrical, thermal, chemical, and mechanical properties. This was conducted by subjecting sample specimens to boiling water and sulphuric acid solutions of pH between 1 and 2 for periods up to 6 months, followed by high vacuum drying for 3 months at  $60^{\circ}\text{C}$ , and for another 3 months at  $140^{\circ}\text{C}$ . The latter drying steps were needed to remove the traces of moisture remaining in the samples. It was found that the specimens subjected to water and acid reflux

Table 4

Glass transition and thermal degradation temperatures of EP90 composites

EP/EG/CB	$T_g$ ( $^{\circ}\text{C}$ )	$T_1$ ( $^{\circ}\text{C}$ )	$T_2$ ( $^{\circ}\text{C}$ )
100/0/0	182	390	424
50/50/0	177	389	414
50/45/5	174	370	403
40/60/0	179	385	415
40/55/5	179	368	402

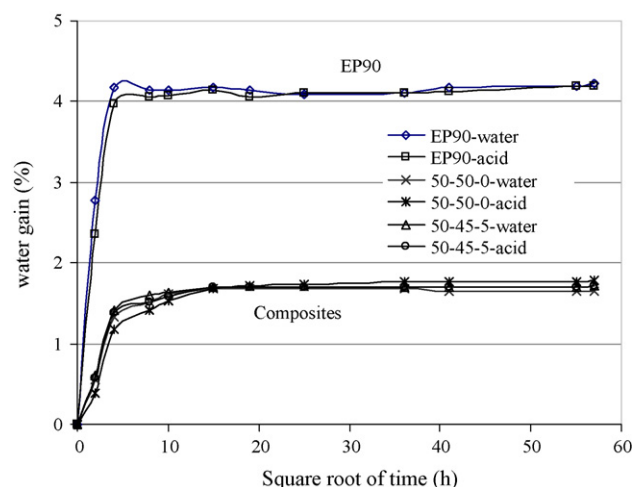


Fig. 8. Water absorption profiles of EP90 resin and composites during water and acid reflux.

presented no discernible difference in material dimension and surface appearance. The thicknesses of the samples recorded before and after reflux and drying steps did not show any change indicating that specimens had excellent dimensional stability.

One can see from water absorption profile in Fig. 8 that water uptake increased linearly with time in the early periods and reached a plateau after about 100 h, indicating that the samples were saturated by water after 100 h. The monotonic increase of water uptake and reaching a plateau suggests that water absorption in both EP resin and composites followed Fickian diffusion behavior at the temperature of  $100^{\circ}\text{C}$ , although Zhou and coworkers [28–31] reported Fickian water diffusion behavior for graphite/epoxy composites at much lower reflux temperatures  $\sim 45^{\circ}\text{C}$  and non-Fickian diffusion behavior at reflux temperature greater than  $90^{\circ}\text{C}$ . It is seen from Fig. 8 that the maximum water uptake was about 1.7–1.8% by weight for composites, compared to 4.2–4.3% by weight for neat epoxy resin. A reduction in total water absorption in composites can be attributed to the presence of EG and CB fillers.

### 3.5. Mechanical properties

Bipolar plates must possess good mechanical properties to support thin membranes and electrodes, and to withstand high clamping forces for the stack assembly. However, high loading of conductive fillers required to reach high electrical conductivity, may also introduce voids and defects in the resulting composites, especially if the filler loading is higher than a critical volume concentration, known in additive industry as the critical pigment volume concentration [26,32–34]. In view of this, it is difficult to obtain simultaneously high electrical conductivity and sufficient mechanical strength from the same materials. Recall that in this work a solution intercalation method was used to mix the epoxy and fillers without shear force, which to some extent preserved the layered and network structures of EG particles in the composites as shown in Fig. 9. Also, low viscosity allowed epoxy resins and the curing agent to penetrate into the EG gallery and fill the micro- and macro-pores of the EG particles. In addition,

Table 5  
Mechanical properties of epoxy composites compared with DOE target values

EP90/EG/CB	Flexural modulus (MPa)	Flexural strength (MPa)	Tensile strength (MPa)	Impact strength (J/m)
60/40/0	$1.77 \times 10^4$	61	40	
60/35/5	$0.75 \times 10^4$	40	29	
50/50/0	$2.08 \times 10^4$	72	45	173
50/45/5	$1.49 \times 10^4$	44	26	144
40/60/0	$2.66 \times 10^4$	82	31	
40/55/5	$1.76 \times 10^4$	56	25	
DOE target		59	41	40.5

DOE target values are quoted from Refs. [5,6].

the large pressure applied during epoxy curing led to reduction of the voids and defects. Furthermore, synergistic combination of EG and CB allowed substantial reduction of total filler loading to reach high electrical conductivity. Thus several measures were taken in composite preparation method to eliminate possible sources of voids and defects. Table 5 lists the mechanical properties of the composites. It is seen that impact strengths of the samples, 173 and 144 J m<sup>-1</sup> for composites epoxy/EG/CB (50/50/0) and epoxy/EG/CB (50/45/5) respectively, exceeds the DOE target value of 40.5 J m<sup>-1</sup> [5,6]. The flexural strengths of epoxy composites without CB are also higher than the DOE target value of 59 MPa [5,6], although the flexural strengths decreased with the addition of 5 wt% CB. The tensile strengths of epoxy composites are lower than the DOE target value of 41 MPa except in the case of 50:50:0 ratio of EP90/EG/CB. The mechanical properties of data presented in Table 5 also compares well with the data reported in literature. For example, composites of PPS and polyethyleneterephthalate with graphite and carbon nanofibers provided in-plane and through-plane conductivity of 230–271 and 18–25 S cm<sup>-1</sup>, respectively [2]. In addition, PPS composites provide flexural strengths of 96 MPa and tensile strength of 58 MPa [2].

The mechanical properties of composites did not change appreciably when refluxed in boiling acid solution and in water for a period of 6 months. Specifically, the values of storage modulus of specimens before and after acid and water reflux were obtained using dynamic mechanical analyzer at 30 °C and

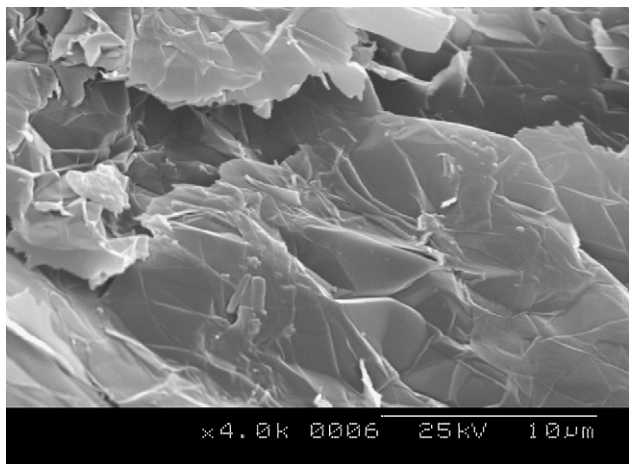


Fig. 9. Morphology of the composites showing layered and network structure of EG.

a frequency of 1 Hz. It was found that a composite with 50 parts by weight epoxy, 46 parts by weight expanded graphite, and 4 parts by weight carbon black provided storage modulus  $9.5 \times 10^3$  MPa before reflux,  $8.7 \times 10^3$  MPa after reflux in water, and  $7.8 \times 10^3$  MPa after reflux in acid solution. Note that unfilled epoxy showed storage modulus values of  $2 \times 10^3$  MPa,  $2.1 \times 10^3$  MPa, and  $1.8 \times 10^3$  MPa respectively before reflux, after reflux in water, and after reflux in acid solution. In view of these and the data presented in Table 5, it can be inferred that the composite materials developed in this study offer many of the attributes required of bipolar plates.

#### 4. Conclusions

The study showed that highly conductive epoxy composites can be developed using synergistic combinations of EG and CB as conductive fillers. The data on electrical conductivity, thermal and mechanical properties, and stability against long exposure to acid solution indicate that these composites will be very suitable for bipolar plates in PEM hydrogen fuel cells. Specifically, the composites developed in this study exceeded many specifications set by the industry, e.g. these provide in-plane conductivity  $\sim 200$ – $500$  S cm<sup>-1</sup>, high through-plane conductivity of 77 S cm<sup>-1</sup>, low area specific resistance, high glass transition temperatures ( $T_g \sim 180$  °C) and high thermal degradation temperatures ( $T_2 \sim 415$  °C).

#### References

- [1] J. Larminie, A. Dicks, Fuel Cell Systems Explained, John Wiley & Sons Ltd., Wiltshire, 2003, pp. 1–108.
- [2] J. Huang, D.G. Baird, J.E. McGrath, J. Power Sources 150 (2005) 110–119.
- [3] A. Heinzl, F. Mahlendorf, O. Niemzig, C. Kreuz, J. Power Sources 131 (2004) 35–40.
- [4] X.G. Li, I. Sabir, Int. J. Hydrogen Energy 30 (2005) 359–371.
- [5] W. Vielstich, H.A. Gasteiger, A. Lamm (Eds.), Handbook of Fuel Cells—Fundamentals, Technology and Applications, vol. 3: Fuel Cell Technology and Applications, Wiley & Sons, New York, 2003, pp. 286–293.
- [6] J.G. Clulow, F.E. Zappitelli, C.M. Carlstrom, J.I.L. Zemsky, D.N. Busick, M.S. Wilson, Fuel Cell Technology: Opportunities and Challenges Topical Conference Proceedings, AIChE Spring National Meeting, New Orleans, LA, March 10–14, 2002, pp. 417–425.
- [7] A.-M. Lafront, E. Ghali, A.T. Morales, Electrochim. Acta 52 (2007) 5076–5085.
- [8] H. Tawfik, Y. Hung, D. Mahajan, J. Power Sources 163 (2007) 755–767.
- [9] Y. Show, M. Miki, T. Nakamura, Diam. Relat. Mater. 16 (2007) 1159–1161.
- [10] Y. Wang, D.O. Northwood, J. Power Sources 163 (2006) 500–508.

- [11] S.-H. Wang, J. Peng, W.-B. Lui, J.-S. Zhang, *J. Power Sources* 162 (2006) 486–491.
- [12] I.E. Paulauskas, M.P. Brady, H.M. Meyer III, R.A. Buchanan, L.R. Walker, *Corros. Sci.* 48 (2006) 3157–3171.
- [13] B. Cunningham, D.G. Baird, *J. Mater. Chem.* 16 (2006) 4358–4388.
- [14] F. Barbir, J. Braun, J. Neutzler, *J. New Mater. Electrochem. Sys.* 2 (1999) 197–200.
- [15] H.-C. Kuan, C.-C.M. Ma, K.H. Chen, S.-M. Chen, *J. Power Sources* 134 (2004) 7–17.
- [16] A. Kumar, R.G. Reddy, *J. Power Sources* 129 (2004) 62–67.
- [17] E.A. Cho, U.-S. Jeon, H.Y. Ha, S.-A. Hong, I.-H. Oh, *J. Power Sources* 125 (2004) 178–182.
- [18] B. Cunningham, D.G. Baird, *J. Power Sources* 168 (2007) 418–425.
- [19] T.M. Besmann, J.W. Klett, J.J. Henry Jr., E. Lara-Curzio, *J. Electrochem. Soc.* 147 (2000) 4083–4086.
- [20] J.-K. Kuo, C.-K. Chen, *J. Power Sources* 162 (2006) 207–214.
- [21] J.-F. Zou, Z.-Z. Yu, Y.-X. Pan, X.-P. Fang, Y.-C. Ou, *J. Polym. Sci. Part B: Polym. Phys.* 40 (2002) 954–963.
- [22] W. Zheng, S.-C. Wong, *Comp. Sci. Tech.* 63 (2003) 225–235.
- [23] M.L. Clingerman, E.H. Weber, J.A. King, K.H. Schulz, *Polym. Compos.* 23 (2002) 911–924.
- [24] J.B. Donnet, R.C. Bansal, M.J. Wang (Eds.), *Carbon Black, Science and Technology*, Dekker, New York, 1993, pp. 1–66.
- [25] R. Blunk, F. Zhong, J. Owens, *J. Power Sources* 159 (2006) 533–542.
- [26] V. Meha, J.S. Copper, *J. Power Sources* 114 (2003) 32–53.
- [27] S. Gottesfeld, T. Zawodzinski, *Adv. Electrochim. Sci. Eng.* 5 (1997) 195–301.
- [28] J. Zhou, J.P. Lucas, *Polymer* 40 (1999) 5505–5512.
- [29] J. Zhou, J.P. Lucas, *Polymer* 40 (1999) 5513–5522.
- [30] J. Zhou, J.P. Lucas, *J. Thermoplast. Compos. Mater.* 9 (1996) 316–328.
- [31] E.E. Shin, R.J. Morgan, J. Zhou, J. Lincoln, R. Jurek, D.B. Curliss, *J. Thermoplast. Compos. Mater.* 13 (2000) 40–57.
- [32] E.K. Sichel, *Carbon Black—Polymer Composites*, Marcel Dekker, New York, 1982, pp. 163–187.
- [33] B. Wessling, *Polym. Eng. Sci.* 31 (2004) 1200–1206.
- [34] G. Wypych, *Handbook of Fillers*, ChemTec. Pub., New York, 2000, pp. 241–304.